HHS Public Access

Author manuscript

Mol Psychiatry. Author manuscript; available in PMC 2017 April 26.

Published in final edited form as:

Mol Psychiatry. 2017 July ; 22(7): 981–989. doi:10.1038/mp.2016.189.

Lysosomal dysfunction in the brain of a mouse model with intraneuronal accumulation of carboxyl terminal fragments of the amyloid precursor protein

Gurjinder Kaur, PhD[1], **Monika Pawlik, PhD**[1], **Sam E. Gandy, MD, PhD**[2], **Michelle E. Ehrlich, MD**[3], **John F. Smiley, PhD**[1,4], and **Efrat Levy, PhD**[1,4,5]

[1]Nathan S. Kline Institute, Orangeburg, NY, USA

[2]Departments of Neurology and Psychiatry, and Alzheimer's Disease Research Center, Icahn School of Medicine at Mount Sinai, New York, and James J. Peters Veterans Affairs Medical Center, Bronx, NY, USA

[3]Departments of Neurology and Pediatrics, Icahn School of Medicine at Mount Sinai, New York, NY, USA

[4]Department of Psychiatry, NYU Langone Medical Center, New York, NY, USA

[5]Department of Biochemistry and Molecular Pharmacology, NYU Langone Medical Center, New York, NY, USA

Abstract

Recent data suggest that intraneuronal accumulation of metabolites of the amyloid β precursor protein (APP) is neurotoxic. We observed that transgenic mice overexpressing in neurons a human APP gene harboring the APP^{E693Q} (Dutch) mutation have intraneuronal lysosomal accumulation of APP carboxyl-terminal fragments (APP-CTFs) and oligomeric amyloid β (oAβ) but no histological evidence of amyloid deposition. Morphometric quantification using the lysosomal marker protein 2 (LAMP-2) immunolabeling showed higher neuronal lysosomal counts in brain neurons of 12 months old APP^{E693Q} as compared to age-matched non-transgenic littermates, and Western blots showed increased lysosomal proteins including LAMP-2, cathepsin D and LC3. At 24 months of age, these mice also exhibited an accumulation of α-synuclein in the brain, along with increased conversion of LC3-I to LC3-II, an autophagosomal/autolysosomal marker. In addition to lysosomal changes at 12 months of age, these mice developed cholinergic neuronal loss in the basal forebrain, GABAergic neuronal loss in the cortex, hippocampus and basal forebrain, and gliosis and microgliosis in the hippocampus. These findings suggest a role for the intraneuronal accumulation of oAβ and APP-CTFs and resultant lysosomal pathology at early stages of Alzheimer's disease-related pathology.

Corresponding author: Efrat Levy, Nathan S. Kline Institute, 140 Old Orangeburg Road, Orangeburg, NY 10962. Phone: (845) 398 5540; Fax: (845) 398 5422; elevy@nki.rfmh.org.

Conflict of Interest: The authors declare no competing financial interests in relation to the work described.

Keywords

carboxyl-terminal fragments of APP; oligomeric amyloid β; lysosomes; neurodegeneration

Introduction

Alzheimer's disease (AD) is a neurodegenerative disorder that typically begins with mild short-term memory deficits and culminates in total loss of cognition and executive functions. The neuropathological features of AD include brain parenchymal senile plaques, cerebral amyloid angiopathy (CAA), and neurofibrillary tangles[1]. Hereditary cerebral hemorrhage with amyloidosis-Dutch type (HCHWA-D), a familial form of AD[2–3], is caused by an E693Q substitution in the amyloid β precursor protein (APP)[4]. The disease is characterized by CAA leading to hemorrhagic strokes[5–6], as well as cerebral lesions caused by the hemorrhages[7], non-fibrillar parenchymal deposits of amyloid β (Aβ)[6, 8–10], and dementia[11–12]. Aβ harboring the Dutch substitution at position 22 has been associated with enhanced aggregation and oligomerization[13–14] and reduced clearance as compared to wild-type Aβ[15–16].

Two mouse lines overexpressing the E693Q-substituted human APP under the neuron-specific Thy1.1 expression cassette were generated[16–17]. Similar to the brains of HCHWA-D patients[18], higher Aβ40 to Aβ42 ratio was observed in the brains of the APP^{E693Q} transgenic mice as compared to non-transgenic littermates[16–17]. It was shown that neurons in the brain of 12 months old APP^{E693Q} mice contain vesicles immunopositive for antibodies that interact with full-length APP (flAPP), APP-CTFs, and Aβ[17]. Aβ has been shown to exist in different forms, including soluble Aβ monomers and oligomers, as well as insoluble amyloid fibrils and multiple studies have documented the correlation between Aβ pathology and cognitive decline in AD[19–21]. Synaptic dysfunction and neuronal degeneration have been demonstrated in the brains lacking amyloid plaques and CAA during the early stages of AD, and several lines of evidence have suggested that soluble oligomers of Aβ, but not monomers, cause the synaptic dysfunction and neurodegeneration in the brains of AD patients and animal models[19–21]. In addition to Aβ, APP carboxyl-terminal fragments (APP-CTFs) have been shown to exhibit cytotoxicity in the absence of amyloid deposition in the brain[22–38]. APP^{E693Q} mice have behavioral deficits at ages when APP metabolites accumulate within neurons but no fibrillar amyloid deposits are detectable in either brain vasculature or parenchyma[17, 39–41].

While the cellular events triggered by neurotoxic oAβ accumulation that lead to synaptic deficits may vary in different forms of AD, data suggest that neuronal endocytic-lysosomal alterations are either an underlying pathological mechanism in the disease or a maladaptive response of neurons to other disease stresses in AD[42–46]. Given that endosomal abnormalities were reported in cerebral endothelia in the brain of HCHWA-D patients[43] and that we have documented intraneuronal punctate accumulation of APP metabolites in cortical and hippocampal brain regions of APP^{E93Q} transgenic mice[17], we investigated the endosomal-lysosomal pathway in the brain of these APP^{E93Q} transgenic mice. Here we

demonstrate the intraneuronal lysosomal accumulation of APP-CTFs associated with intraneuronal lysosomal abnormalities and neuronal loss in the absence of fibrillar Aβ.

Materials and methods

Animals

A breeding colony of APP^{E693Q} mice[17] on C57BL/6J background was maintained at Nathan S. Kline Institute for Psychiatric Research. Both male and female APP^{E693Q} transgenic mice and littermate controls were studied at 12 and 24 months of age. No gender differences between the genotypes were found. All animal procedures were performed following the National Institutes of Health guidelines with approval from the Institutional Animal Care and Use Committee at the Nathan S. Kline Institute for Psychiatric Research. All the experiments were performed with a sample size of 4–5 mice per genotype per age. The sample size was determined on the basis of findings from our previous APP^{E693Q} transgenic mouse studies[17].

Thioflavin S staining and immunocytochemistry

For all histological procedures, identification cards were coded to render the experimenter blind to the sex and genotype of each subject. Mice were anesthetized with ketamine (50 g/kg)/xylazine (5 mg/kg) and transcardially perfusion-fixed with 4% paraformaldehyde in 0.1 M sodium cacodylate buffer[47]. To detect fibrillar amyloid deposits, brain sections from 12 and 24 months old mice were slide-mounted and immersed in a solution of filtered 1% thioflavin S in ddH_20 for 10 minutes (Sigma Aldrich, St. Louis, MO), rinsed (×3) for 1 minute in ddH_20 and subsequently cover-slipped with Vectashield mounting medium (Vector Laboratories, Inc., Burlingame, CA). Immunolabeling was performed using 4G8 antibody (which recognizes flAPP/APP-CTF/Aβ; 1:200; Covance ImmunoTechnologies, Denver, PA; Cat # SIG-39220), C1/6.1 to the carboxyl-terminal cytoplasmic domain of APP (1:100; provided by Dr. Paul M. Mathews). 22C11 antibody (which recognizes full length and soluble amino terminal fragment of APP, sAPP) (1:200; EMD Millipore, Billerica, MA; Cat # MAB 348), anti-glial fibrillary acidic protein (GFAP) (1:500; Dako, Carpinteria, CA; Cat # Z0334), anti-Iba1 (1:500, Wako Chemicals, Richmond, VA; Cat # 019-1974), anti-rab5a (1:100, Santa Cruz Biotechnology, Santa Cruz, CA; Cat # SC-309), anti-cathepsin D (Cat D) (1:500; Scripps, San Diego, CA; Cat # 90236), anti-LC3 (1:500; Novus Biologicals, Littleton, CO; Cat # NB600-1384), anti-lysosomal marker protein 2 (LAMP-2) (1:100; Developmental Studies Hybridoma Bank, Iowa City, Iowa; Cat # 93S), and anti-ChAT antibody (1:500; Millipore Corporation, Billerica, MA; Cat # AB144P) antibodies. Double immunofluorescent labeling was performed to identify coincidence of localization of flAPP/APP-CTFs/Aβ using 4G8 (1:200) or flAPP/APP-CTFs using antibody to the carboxyl-terminal cytoplasmic domain of APP using C1/6.1[48] (1:100) with antibody to the lysosomal marker LAMP-2 (1:100). Anti-parvalbumin (PV) (1:5000; Swant technologies, Switzerland; Cat # PV25) staining was performed to detect GABAergic interneurons. Secondary antibodies used were: fluorescence-conjugated anti-rabbit and anti-mouse antibody (Invitrogen Corporation, Carlsbad, CA), and anti-sheep antibody (1:500; Invitrogen, Grand Island, NY).

PV-positive GABAergic interneurons were quantified in the hippocampus of 4 individual brain sections per mouse, 5 mice per genotype, at the age of 12 months using ImageJ (NIH, USA). For lysosomal quantification, approximately 30 neurons per mouse, 4 mice per genotype, were analyzed and LAMP-2 signal was measured using ImageJ randomly by a genotype-blinded observer[47]. LAMP-2 labeled brain sections were further stained with Nissl (Neurotrace) (1:100; Molecular probes, Eugene, OR) to quantify lysosomes in the large neurons of the MSN, counting approximately 30 neurons per mouse, 4 mice per genotype. LAMP-2 signal was measured using ImageJ. Qualitative analysis of GFAP- or Iba1-positive staining was performed on 4 individual brain sections per mouse, 5 mice per genotype, at the ages of 12 and 24 months.

Optical fractionator procedure

The number of immunofluorescence-labeled ChAT cells in the MSN was estimated using the optical fractionator method[49], utilizing ImageJ software as previously described[50]. Briefly, the MSN was sampled in every 3rd consecutive 40 μm-thick vibratome section rostral to the anterior commissure. A grid of optical disector sampling sites with 0.25 mm spacing was placed on each section. At each sampling site, a 40x oil-immersion objective with 1.3 numerical aperture was used to collect a z-stack of fifteen 3-μm spaced images starting at a focal plane just beneath the tissue surface. Cell counting was done on 198 × 143 μm counting boxes drawn onto each z-stack, using the top 2 slices as the upper guard zone, the next 10 slices as a 30 μm deep counting box, and the subsequent slices as the lower guard zone. Section thickness (40.5 +/− 1.7 μm mean +/− S.D., n=8 animals), measured in triplicate on each section, showed no evidence of shrinkage from the original 40 μm section thickness. On average, 191 +/− 69 cells were counted per MSN, and the coefficient of error[51] was 0.08 +/− 0.01 (mean +/− S.D.).

Western blot analysis

Mice were anesthetized with ketamine (50 g/kg)/xylazine (5 mg/kg) and brains were rapidly removed over ice. Brains of 12 (n=4) and 24 (n=5) month old mice were snap frozen and stored at −80°C before biochemical analyses. Entorhinal cortices were dissected out from fresh brains of 12 (n=4) and 24 (n=4) month old mice and stored at −80°C. Western blot immunolabeling was performed as previously described[52]. Primary antibodies used were: anti-LAMP-2 (1:1000), anti-Rab4a (1:1000; Santa Cruz Biotechnology, Santa Cruz, CA; Cat # SC-312), anti-Rab5a (1:1000), anti-Rab7 (1:1000; Sigma, St. Louis, MO; Cat # R8779), anti-Rabaptin5 (1:1000; Santa Cruz Biotechnology, Santa Cruz, CA; Cat # SC-6162), anti-LC3 (1:1000), anti-Cat D (1:1000), C1/6.1 (1:1000)[48], anti-mTOR and anti-AKT (phosphorylated and total protein) (1:1000, Cell Signaling Technology, Inc., Danvers, MA; Cat # 2983S and Cat # 9272S respectively), anti-α-synuclein (1:1000; Sigma, St. Louis, MO; Cat # S3062), and anti-β-tubulin (1:10000; Sigma, St. Louis, MO; Cat # T8535). Secondary antibodies used were: HRP conjugated anti-rabbit and mouse antibodies (1:5000; GE Healthcare, Pittsburgh, PA). The protein bands were scanned, optical density was calculated using the Image J, and the ratio of protein intensity to β-tubulin in the same lane was calculated. Western blot analyses were repeated 3 times.

Statistical analyses

Results were evaluated using one-way ANOVA followed by *post hoc* multiple-comparison Bonferroni's tests to determine the disparity among different age groups between the genotypes. Unpaired, two-tailed Student's *t*-test was used to analyze results among genotypes. A p value of $p<0.05$ was considered statistically significant. None of the animals were excluded from analysis. No randomization was used in this study. The data from each group showed similar variance, presented in the study as mean ± SEM.

Results

Lysosomal localization of APP metabolites in the brain of APP^{E693Q} mice

Immunocytochemistry revealed brain region-specific high levels of staining by antibodies to APP and its metabolites in APP^{E693Q} mice as compared with their wild-type (WT) littermate controls. Strong intraneuronal, punctate, 4G8-immuno-positive staining that identifies flAPP, APP-CTFs, and Aβ was detected in the entorhinal and frontoparietal cortices of 12 months old APP^{E693Q} mice as compared to WT mice (Fig 1A). Similarly, robust intraneuronal, punctate staining was observed with C1/6.1, an antibody that binds flAPP and APP-CTFs, in 12 months old APP^{E693Q} mice as compared to WT mice (Fig 1B). Staining with an antibody against the amino-terminus of APP (22C11) that binds both flAPP and amino-terminal soluble fragments of APP (sAPP) showed a lower difference between APP^{E693Q} and WT mice as compared to the staining with 4G8 and C1/6.1 in the brain of the APP^{E693Q} mice (Fig 1C). Dual immunostaining with an antibody to the lysosomal protein LAMP-2 showed that staining with both 4G8 and C1/6.1 was largely localized to lysosomes in the brains of APP^{E693Q} transgenic mice (Fig 1A & B). Compared with the staining with these two antibodies, fewer LAMP-2 lysosomes were stained with 22C11 (Fig 1C). These data indicate the accumulation of APP-CTFs, but not of flAPP or sAPP, in lysosomes in the brain of APP^{E693Q} transgenic mice.

Western blot analysis with the antibody C1/6.1 demonstrated that while there was no change in the expression level of flAPP, APP-CTFs levels were significantly elevated in the brains of 24 months old compared to 12 months old APP^{E693Q} mice (Fig 1D). This reveals accumulation of APP-CTFs in the brains of APP^{E693Q} mice with age, in addition to the previous demonstration of accumulation of oAβ[17, 41]. No fibrillar amyloid deposits were observed in the brains of APP^{E693Q} mice up to 24 months of age (Fig 1E).

Lysosomal pathology in the brain of APP^{E693Q} mice

Immunocytochemical and Western blot analyses were conducted in order to investigate whether accumulation of APP metabolites in neuronal lysosomes affects the endocytic pathway in APP^{E693Q} mouse brains. Immunostaining with an antibody to the early endosomal protein rab5 showed no difference in endosomal size between APP^{E693Q} mice and WT littermate control mice (Fig 2A). Furthermore, no differences were observed in 12 and 24 months old APP^{E693Q} mice by Western blot analysis of hemibrain homogenates with antibodies to the early endosomal marker, rab5a, the rab5 effector protein, rabaptin 5, the late endosomal marker, rab7, and the recycling endosomal marker, rab4a (Fig 2B), suggesting that the endosomal pathway is unaffected.

Immunocytochemistry of lysosomal proteins have shown higher intensity staining and higher number of LAMP-2-positive vesicles per neuron in the entorhinal and frontoparietal cortices in the brains of 12 months old APP^{E693Q} compared to WT mice (Fig 1A, B, & C & Fig 2C). Quantification of LAMP-2 positive lysosomes in the frontoparietal and entorhinal cortices revealed higher lysosomal counts (Fig 2D) in brain neurons of APP^{E693Q} mice as compared to WT controls mice. Similar to LAMP-2, higher intensity staining and higher number of stained vesicles were observed with the antibody to the lysosomal hydrolase Cat D in the entorhinal cortices of 12 months old APP^{E693Q} as compared to WT mice (Fig 2G). While Western blot analysis of entorhinal cortical homogenates of 12 months old mice with antibodies to LAMP-2 and Cat D showed a non-significant trend towards greater levels in APP^{E693Q} compared to WT mice, Western blot analysis of entorhinal cortical homogenates of 24 months old mice showed significantly higher levels of LAMP-2, and active Cat D in APP^{E693Q} as compared to WT mice (Fig 2E, F, H & I). These data show that immunocytochemical staining revealed lysosomal changes in specific neuronal populations, apparent already in the brain of 12 months old transgenic mice, whereas Western blot analysis of brain tissue that contains multiple cellular populations, including astrocytes and microglia, did not show lysosomal changes at 12 months of old. Significantly higher levels of lysosomal proteins were observed by Western blot analysis of entorhinal cortices of APP^{E693Q} compared to WT mice at 24 months of age. These data reveal an age-dependent increase in lysosomal pathology in entorhinal cortical neurons of APP^{E693Q} mice. While similar changes in the lysosomal markers LAMP-2 and Cat D were observed in multiple brain regions, the entorhinal cortex was the region most affected by lysosomal pathology in the brain of APP^{E693Q} mice. Furthermore, immunostaining and Western blots showed higher LC3 expression levels in the entorhinal cortex of APP^{E693Q} as compared to WT mice at 24 months of age (Fig 3A–C). Additionally, higher levels of conversion from LC3-I to LC3-II were observed in APP^{E693Q} mice as compared to WT littermate controls (Fig 3D). While higher levels of LC3 and conversion from LC3-I to LC3-II were observed in brain homogenate of APP^{E693Q} mice as compared to WT littermate controls, study of the mammalian target of rapamycin (mTOR) signaling pathway to test its involvement in autophagic abnormalities in APP^{E693Q} mice did not show differences in the phosphorylation of proteins such as P70S6K, AKT, and mTOR between APP^{E693Q} mice and littermate controls (Fig 3E), suggesting lysosomal dysfunction, but not autophagic pathology that leads to defective clearance of neuronal autophagic substrates in APP^{E693Q} mice.

Based on recent indications that impaired lysosomal clearance may also be associated with accumulation of neurodegeneration-related proteins, including α-synuclein, in an APP transgenic mouse model[53], we sought to determine the levels of α-synuclein in the brains of APP^{E693Q} mice. Western blot analysis of 24 months old APP^{E693Q} mouse brains exhibited higher levels of α-synuclein as compared to WT mice (Fig 3F & G), supporting impaired lysosomal function.

Cholinergic neuronal loss in the medial septal nucleus (MSN) of APP^{E693Q} mice

Basal forebrain cholinergic neurons (BFCN) are particularly vulnerable to degeneration in AD[54]. We undertook to investigate whether lysosomal abnormality in neurons affects BFCN in the MSN of APP^{E693Q} mice. Comparison of cholinergic neurons in the MSN of

APP^{E693Q} and WT mice by immunostaining with antibody to ChAT revealed lower number of immunopositive cells in APP^{E693Q} mice at 12 months of age as compared to littermate controls (Fig 4A). Using quantitative unbiased stereology, we found that APP^{E693Q} mice had significantly fewer ChAT-positive cells in the MSN as compared to WT mice (Fig 4A & B). We further investigated the lysosomal abnormalities in large neurons of the MSN immunostained with LAMP-2, counter-stained with Nissl (Fig 4C). Quantification of LAMP-2 positive lysosomes in these large septal neurons showed bigger lysosomal size (Fig 4D) in brains of APP^{E693Q} mice as compared to WT controls mice.

Loss of GABAergic interneurons in the brain of APP^{E693Q} mice

Immunostaining of GABAergic interneurons with an antibody to PV has shown that the GABAergic cell population was decreased in the cortex, hippocampus, and MSN areas in 12 months old APP^{E693Q} as compared to WT mice (Fig 4E). PV-positive cells in the hippocampi of APP^{E693Q} and WT mice were quantified revealing a lower number of these inhibitory interneurons in the hippocampus of APP^{E693Q} mice as compared to WT controls (Fig 4F).

Activation of astrocytes and microglia in the brain of APP^{E693Q} mice

In 29 months old mice of the model described by Herzig et al[16], microglial activation demonstrated by Iba-1 immunostaining was observed in the immediate vicinity of amyloid-laden vessels and adjacent areas, and GFAP-positive activated astrocytes were observed in neocortical areas affected by CAA. In the APP^{E693Q} mice studied here we observed higher intensity of GFAP and Iba1 immunostaining, suggesting activated glial and microglial cells in the hippocampus, particularly in the hilus of dentate gyrus and extended to the granular cell layer and corpus callosum (Fig 4G & H) in the absence of amyloid deposition.

Discussion

This study revealed age-dependent intraneuronal accumulation of APP-CTFs in the brains of APP^{E693Q} mice in the absence of cerebral amyloid deposition, in addition to the previously demonstrated intraneuronal accumulation of oAβ[17, 39–41]. Characterization of cellular APP/CTFs accumulation in the absence of parenchymal Aβ deposits and resultant neuropathology are valuable for understanding the pathological determinants of cognitive dysfunction in AD. Our extensive study of the intraneuronal vesicular localization of APP metabolites revealed their accumulation within lysosomes in the brain of 12 months old APP^{E693Q} mice. Dysfunction of lysosomes containing APP-CTFs and/or oAβ aggregates was demonstrated by the observation of higher staining intensity of LAMP-2 and increased numbers of enlarged LAMP-2 positive lysosomes in neurons dually stained with antibodies to flAPP/APP-CTFs/Aβ of 12 months old APP^{E693Q} as compared to WT controls. These data suggest the aggregation of LAMP-2 in lysosomes due to lysosomal dysfunction. Neurons in the brains of APP^{E693Q} mice also had higher levels of the lysosomal hydrolase Cat D. A previous study showed no accumulation of soluble LC3, p62, or α-synuclein in the brains of APP^{E693Q} mice at 6 months of age[41], suggesting an age-dependent lysosomal dysfunction due to the ineffective clearance of APP metabolites. The lysosomal abnormality became more severe at an older age, as revealed by the intraneuronal accumulation of the

autophagosomal/autolysosomal marker LC3 as well as by the increased conversion of LC3-I into LC3-II in entorhinal cortical neurons at 24 months of age. These data suggest early mobilization of the lysosomal system, followed by delayed turnover of intra-lysosomal proteins such as LC3-II that is normally rapidly degraded after fusion of autophagosomes with lysosomes. Additionally, we found increased α-synuclein in lysosomes of 24 month-old APP^{E693Q} mice. α-synuclein forms insoluble fibrils under pathological conditions in Parkinson's disease, dementia with Lewy bodies[55–56], and accumulates in the cortex of 30–50% AD patients[57]. These data show that APP-CTFs accumulation is involved in the age-related changes in the brains of aged mice, and could be a cause of AD-relevant lysosomal dysfunction.

Evidence is mounting from transgenic mice and human patients, indicating that Aβ as well as APP-CTFs accumulate intraneuronally and contribute to AD progression[22–38]. An association between elevated APP-CTFs levels, abnormal endosomal morphology, and BFCN degenerative changes have also been observed in mouse models of familial AD due to other APP mutations[47]. Earlier studies using isotropic fractionator showed no evidence for total neuronal loss in the hippocampus, neocortex, and cerebellum of APP^{E693Q} mice[58], but reduced dendritic arborization of apical dendrites and a decrease in postsynaptic density length in individual hippocampal neurons of 12 months old APP^{E693Q} mice was observed[59]. However, our data show loss of cholinergic neurons in the MSN of our APP^{E693Q} mice. Dysregulated cholinergic signaling is an early hallmark of AD[60]. The severity and magnitude of cholinergic dysfunction appears to depend, at least in part, on age and brain region, in many APP-overexpressing mouse models, including APP23[47, 61–62], TgCRND8[63], Tg2576[64], and APP/PS1K1[65]. The cholinergic fiber loss was attributed to higher Aβ load[66]. However, the observed shrinkage of cholinergic neurons[61] and reduced enzymatic activity in the basal forebrain in 6–8 months old APP23 transgenic mice[62] and the cholinergic degenerative pathology in PDAPP mice[67], indicate the presence of an early cholinergic dysfunction prior to Aβ amyloid deposition. Oligomeric forms of Aβ have been implicated in the reduction in ChAT activity[60] and loss of cholinergic innervation in the neocortex[68], preceding the loss of cholinergic neurons commonly observed in AD brains. However, the data presented here suggest that the neuronal lysosomal dysfunction in MSN cholinergic neurons and cortical regions of APP^{E693Q} mice is due at least in part to the accumulation of APP-CTFs.

Besides showing significant loss of cholinergic cells in the MSN, 12 months old APP^{E693Q} mice also showed GABAergic neurotransmission deficits, similar to other APP transgenic mice, including TgCRND8[69], AbPPdE9[70], and J20 transgenic mice[71]. Both cholinergic and GABAergic cell loss in the brain of these transgenic mice, in the absence of parenchymal and vascular β amyloid deposition, implies a role for intracellular accumulation of APP-CTFs/oAβ in neuronal degeneration and subsequent impaired spatial learning and memory, novel object recognition, and increased anxiety in APP^{E693Q} transgenic mice[17, 39–41].

In conclusion, our results suggest that an age-dependent intraneuronal accumulation of APP-CTFs and oAβ initiates a cascade of pathogenic events, including lysosomal dysfunction in vulnerable brain regions and leads to inflammatory activation, cholinergic and GABAergic

neuronal loss in transgenic mice overexpressing human APP gene harboring the E693Q mutation, leading to memory deficits.

Acknowledgments

National Institutes of Health, Alzheimer's association.

References

1. Hardy J, Selkoe DJ. The amyloid hypothesis of Alzheimer's disease: progress and problems on the road to therapeutics. Science. 2002; 297:353–356. [PubMed: 12130773]
2. Gudmundsson G, Hallgrimsson J, Jonasson TA, Bjarnason O. Hereditary cerebral haemorrhage with amyloidosis. Brain. 1972; 95:387–404. [PubMed: 4655034]
3. Haan J, Roos RA, Briet PE, Herpers MJ, Luyendijk W, Bots GT. Hereditary cerebral hemorrhage with amyloidosis--Dutch type. Clin Neurol Neurosurg. 1989; 91:285–290. [PubMed: 2555088]
4. Levy E, Carman MD, Fernandez-Madrid IJ, Power MD, Lieberburg I, van Duinen SG, et al. Mutation of the Alzheimer's disease amyloid gene in hereditary cerebral hemorrhage, Dutch type. Science. 1990; 248:1124–1126. [PubMed: 2111584]
5. Wattendorff AR, Bots GT, Went LN, Endtz LJ. Familial cerebral amyloid angiopathy presenting as recurrent cerebral haemorrhage. J Neurol Sci. 1982; 55:121–135. [PubMed: 7131028]
6. Luyendijk W, Bots GT, Vegter-van der Vlis M, Went LN, Frangione B. Hereditary cerebral haemorrhage caused by cortical amyloid angiopathy. J Neurol Sci. 1988; 85:267–280. [PubMed: 3210024]
7. Haan J, Algra PR, Roos RA. Hereditary cerebral hemorrhage with amyloidosis-Dutch type. Clinical and computed tomographic analysis of 24 cases. Arch Neurol. 1990; 47:649–653. [PubMed: 2346393]
8. van Duinen SG, Castano EM, Prelli F, Bots GT, Luyendijk W, Frangione B. Hereditary cerebral hemorrhage with amyloidosis in patients of Dutch origin is related to Alzheimer disease. Proc Natl Acad Sci USA. 1987; 84:5991–5994. [PubMed: 3475718]
9. Haan J, Roos RA, Algra PR, Lanser JB, Bots GT, Vegter-Van der Vlis M. Hereditary cerebral haemorrhage with amyloidosis--Dutch type. Magnetic resonance imaging findings in 7 cases. Brain. 1990; 113:1251–1267. [PubMed: 2245295]
10. Coria F, Castano EM, Frangione B. Brain amyloid in normal aging and cerebral amyloid angiopathy is antigenically related to Alzheimer's disease β-protein. Am J Pathol. 1987; 129:422–428. [PubMed: 3322021]
11. Haan J, Lanser JB, Zijderveld I, van der Does IG, Roos RA. Dementia in hereditary cerebral hemorrhage with amyloidosis-Dutch type. Arch Neurol. 1990; 47:965–967. [PubMed: 2396937]
12. Cohn-Hokke PE, Wong TH, Rizzu P, Breedveld G, van der Flier WM, Scheltens P, et al. Mutation frequency of PRKAR1B and the major familial dementia genes in a Dutch early onset dementia cohort. J Neurol. 2014; 261:2085–2092. [PubMed: 25108559]
13. Wisniewski T, Ghiso J, Frangione B. Peptides homologous to the amyloid protein of Alzheimer's disease containing a glutamine for glutamic acid substitution have accelerated amyloid fibril formation. Biochem Biophys Res Commun. 1991; 179:1247–1254. [PubMed: 1681804]
14. Miravalle L, Tokuda T, Chiarle R, Giaccone G, Bugiani O, Tagliavini F, et al. Substitutions at codon 22 of Alzheimer's Aβ peptide induce diverse conformational changes and apoptotic effects in human cerebral endothelial cells. J Biol Chem. 2000; 275:27110–27116. [PubMed: 10821838]
15. Fraser PE, Nguyen JT, Inouye H, Surewicz WK, Selkoe DJ, Podlisny MB, et al. Fibril formation by primate, rodent, and Dutch-hemorrhagic analogues of Alzheimer amyloid β-protein. Biochemistry. 1992; 31:10716–10723. [PubMed: 1420187]
16. Herzig MC, Winkler DT, Burgermeister P, Pfeifer M, Kohler E, Schmidt SD, et al. Aβ is targeted to the vasculature in a mouse model of hereditary cerebral hemorrhage with amyloidosis. Nat Neurosci. 2004; 7:954–960. [PubMed: 15311281]

17. Gandy S, Simon AJ, Steele JW, Lublin AL, Lah JJ, Walker LC, et al. Days to criterion as an indicator of toxicity associated with human Alzheimer amyloid-β oligomers. Ann Neurol. 2010; 68:220–230. [PubMed: 20641005]
18. Prelli F, Castano E, Glenner GG, Frangione B. Differences between vascular and plaque core amyloid in Alzheimer's disease. J Neurochem. 1988; 51:648–651. [PubMed: 3292706]
19. Walsh DM, Selkoe DJ. Aβ oligomers - a decade of discovery. J Neurochem. 2007; 101:1172–1184. [PubMed: 17286590]
20. Haass C, Selkoe DJ. Soluble protein oligomers in neurodegeneration: lessons from the Alzheimer's amyloid β-peptide. Nat Rev Mol Cell Biol. 2007; 8:101–112. [PubMed: 17245412]
21. Sengupta U, Nilson AN, Kayed R. The role of amyloid-β oligomers in toxicity, propagation, and immunotherapy. EBioMedicine. 2016; 6:42–49. [PubMed: 27211547]
22. Bertrand E, Brouillet E, Caille I, Bouillot C, Cole GM, Prochiantz A, et al. A short cytoplasmic domain of the amyloid precursor protein induces apoptosis *in vitro* and *in vivo*. Mol Cell Neurosci. 2001; 18:503–511. [PubMed: 11922141]
23. McPhie DL, Golde T, Eckman CB, Yager D, Brant JB, Neve RL. β-Secretase cleavage of the amyloid precursor protein mediates neuronal apoptosis caused by familial Alzheimer's disease mutations. Brain Res Mol Brain Res. 2001; 97:103–113. [PubMed: 11744168]
24. Jiang Y, Mullaney KA, Peterhoff CM, Che S, Schmidt SD, Boyer-Boiteau A, et al. Alzheimer's-related endosome dysfunction in Down syndrome is Aβ-independent but requires APP and is reversed by BACE-1 inhibition. Proc Natl Acad Sci USA. 2010; 107:1630–1635. [PubMed: 20080541]
25. Lauritzen I, Pardossi-Piquard R, Bauer C, Brigham E, Abraham JD, Ranaldi S, et al. The β-secretase-derived C-terminal fragment of βAPP, C99, but not Aβ, is a key contributor to early intraneuronal lesions in triple-transgenic mouse hippocampus. J Neurosci. 2012; 32:16243–16255a. [PubMed: 23152608]
26. Tamayev R, Matsuda S, Arancio O, D'Adamio L. β- but not γ-secretase proteolysis of APP causes synaptic and memory deficits in a mouse model of dementia. EMBO Mol Med. 2012; 4:171–179. [PubMed: 22170863]
27. Nhan HS, Chiang K, Koo EH. The multifaceted nature of amyloid precursor protein and its proteolytic fragments: friends and foes. Acta Neuropathol. 2015; 129:1–19. [PubMed: 25287911]
28. Xu W, Fitzgerald S, Nixon RA, Levy E, Wilson DA. Early hyperactivity in lateral entorhinal cortex is associated with elevated levels of AβPP metabolites in the Tg2576 mouse model of Alzheimer's disease. Exp Neurol. 2015; 264:82–91. [PubMed: 25500142]
29. Kim S, Sato Y, Mohan PS, Peterhoff C, Pensalfini A, Rigoglioso A, et al. Evidence that the rab5 effector APPL1 mediates APP-βCTF-induced dysfunction of endosomes in Down syndrome and Alzheimer's disease. Mol Psychiatry. 2016; 21:707–716. [PubMed: 26194181]
30. Cavanagh C, Colby-Milley J, Bouvier D, Farso M, Chabot JG, Quirion R, et al. βCTF-correlated burst of hippocampal TNFα occurs at a very early, pre-plaque stage in the TgCRND8 mouse model of Alzheimer's disease. J Alzheimers Dis. 2013; 36:233–238. [PubMed: 23579326]
31. Jiang Y, Rigoglioso A, Peterhoff CM, Pawlik M, Sato Y, Bleiwas C, et al. Partial BACE1 reduction in a Down syndrome mouse model blocks Alzheimer-related endosomal anomalies and cholinergic neurodegeneration: role of APP-CTF. Neurobiol Aging. 2016; 39:90–98. [PubMed: 26923405]
32. Neve RL, Robakis NK. Alzheimer's disease: a re-examination of the amyloid hypothesis. Trends Neurosci. 1998; 21:15–19. [PubMed: 9464679]
33. Tamayev R, D'Adamio L. Inhibition of γ-secretase worsens memory deficits in a genetically congruous mouse model of Danish dementia. Mol Neurodegener. 2012; 7:19. [PubMed: 22537414]
34. Bach JH, Chae HS, Rah JC, Lee MW, Park CH, Choi SH, et al. C-terminal fragment of amyloid precursor protein induces astrocytosis. J Neurochem. 2001; 78:109–120. [PubMed: 11432978]
35. Devi L, Ohno M. Mitochondrial dysfunction and accumulation of the β-secretase-cleaved C-terminal fragment of APP in Alzheimer's disease transgenic mice. Neurobiol Dis. 2012; 45:417–424. [PubMed: 21933711]

36. Lu DC, Rabizadeh S, Chandra S, Shayya RF, Ellerby LM, Ye X, et al. A second cytotoxic proteolytic peptide derived from amyloid β-protein precursor. Nat Med. 2000; 6:397–404. [PubMed: 10742146]
37. Sopher BL, Fukuchi K, Smith AC, Leppig KA, Furlong CE, Martin GM. Cytotoxicity mediated by conditional expression of a carboxyl-terminal derivative of the β-amyloid precursor protein. Brain Res Mol Brain Res. 1994; 26:207–217. [PubMed: 7854049]
38. Yankner BA, Dawes LR, Fisher S, Villa-Komaroff L, Oster-Granite ML, Neve RL. Neurotoxicity of a fragment of the amyloid precursor associated with Alzheimer's disease. Science. 1989; 245:417–420. [PubMed: 2474201]
39. Kim SH, Steele JW, Lee SW, Clemenson GD, Carter TA, Treuner K, et al. Proneurogenic Group II mGluR antagonist improves learning and reduces anxiety in Alzheimer Aβ oligomer mouse. Mol Psychiatry. 2014; 19:1235–1242. [PubMed: 25113378]
40. Knight EM, Williams HN, Stevens AC, Kim SH, Kottwitz JC, Morant AD, et al. Evidence that small molecule enhancement of β-hexosaminidase activity corrects the behavioral phenotype in Dutch APP(E693Q) mice through reduction of ganglioside-bound Aβ. Mol Psychiatry. 2015; 20:109–117. [PubMed: 25349165]
41. Knight EM, Kim SH, Kottwitz JC, Hatami A, Albay R, Suzuki A, et al. Effective anti-Alzheimer Aβ therapy involves depletion of specific Aβ oligomer subtypes. Neurol Neuroimmunol Neuroinflamm. 2016; 3:e237. [PubMed: 27218118]
42. Cataldo AM, Peterhoff CM, Troncoso JC, Gomez-Isla T, Hyman BT, Nixon RA. Endocytic pathway abnormalities precede amyloid β deposition in sporadic Alzheimer's disease and Down syndrome: differential effects of APOE genotype and presenilin mutations. Am J Pathol. 2000; 157:277–286. [PubMed: 10880397]
43. Cataldo A, Rebeck GW, Ghetri B, Hulette C, Lippa C, Van Broeckhoven C, et al. Endocytic disturbances distinguish among subtypes of Alzheimer's disease and related disorders. Ann Neurol. 2001; 50:661–665. [PubMed: 11706973]
44. Ginsberg SD, Alldred MJ, Counts SE, Cataldo AM, Neve RL, Jiang Y, et al. Microarray analysis of hippocampal CA1 neurons implicates early endosomal dysfunction during Alzheimer's disease progression. Biol Psychiatry. 2010; 68:885–893. [PubMed: 20655510]
45. Ling D, Magallanes M, Salvaterra PM. Accumulation of amyloid-like Aβ1-42 in AEL (autophagy-endosomal-lysosomal) vesicles: potential implications for plaque biogenesis. ASN Neuro. 2014; 6:e00139. [PubMed: 24521233]
46. Perez SE, He B, Nadeem M, Wuu J, Ginsberg SD, Ikonomovic MD, et al. Hippocampal endosomal, lysosomal, and autophagic dysregulation in mild cognitive impairment: correlation with Aβ and tau pathology. J Neuropathol Exp Neurol. 2015; 74:345–358. [PubMed: 25756588]
47. Choi JH, Kaur G, Mazzella MJ, Morales-Corraliza J, Levy E, Mathews PM. Early endosomal abnormalities and cholinergic neuron degeneration in amyloid-β protein precursor transgenic mice. J Alzheimers Dis. 2013; 34:691–700. [PubMed: 23254640]
48. Mathews PM, Jiang Y, Schmidt SD, Grbovic OM, Mercken M, Nixon RA. Calpain activity regulates the cell surface distribution of amyloid precursor protein. Inhibition of calpains enhances endosomal generation of β-cleaved C-terminal APP fragments. J Biol Chem. 2002; 277:36415–36424. [PubMed: 12087104]
49. West MJ, Slomianka L, Gundersen HJ. Unbiased stereological estimation of the total number of neurons in thesubdivisions of the rat hippocampus using the optical fractionator. Anat Rec. 1991; 231:482–497. [PubMed: 1793176]
50. Smiley JF, Konnova K, Bleiwas C. Cortical thickness, neuron density and size in the inferior parietal lobe in schizophrenia. Schizophr Res. 2012; 136:43–50. [PubMed: 22304984]
51. Dorph-Petersen KA, Nyengaard JR, Gundersen HJ. Tissue shrinkage and unbiased stereological estimation of particle number and size. J Microsc. 2001; 204:232–246. [PubMed: 11903800]
52. Kaur G, Sharma A, Xu W, Gerum S, Alldred MJ, Subbanna S, et al. Glutamatergic transmission aberration: a major cause of behavioral deficits in a murine model of Down's syndrome. J Neurosci. 2014; 34:5099–5106. [PubMed: 24719089]

53. Steele JW, Ju S, Lachenmayer ML, Liken J, Stock A, Kim SH, et al. Latrepirdine stimulates autophagy and reduces accumulation of α-synuclein in cells and in mouse brain. Mol Psychiatry. 2013; 18:882–888. [PubMed: 22869031]
54. Mufson EJ, Ginsberg SD, Ikonomovic MD, DeKosky ST. Human cholinergic basal forebrain: chemoanatomy and neurologic dysfunction. J Chem Neuroanat. 2003; 26:233–242. [PubMed: 14729126]
55. Mezey E, Dehejia A, Harta G, Papp MI, Polymeropoulos MH, Brownstein MJ. α synuclein in neurodegenerative disorders: murderer or accomplice? Nat Med. 1998; 4:755–757. [PubMed: 9662355]
56. Spillantini MG, Schmidt ML, Lee VM, Trojanowski JQ, Jakes R, Goedert M. α-synuclein in Lewy bodies. Nature. 1997; 388:839–840. [PubMed: 9278044]
57. Yue Z, Friedman L, Komatsu M, Tanaka K. The cellular pathways of neuronal autophagy and their implication in neurodegenerative diseases. Biochim Biophys Acta. 2009; 1793:1496–1507. [PubMed: 19339210]
58. Brautigam H, Steele JW, Westaway D, Fraser PE, St George-Hyslop PH, Gandy S, et al. The isotropic fractionator provides evidence for differential loss of hippocampal neurons in two mouse models of Alzheimer's disease. Mol Neurodegener. 2012; 7:58. [PubMed: 23173713]
59. Price KA, Varghese M, Sowa A, Yuk F, Brautigam H, Ehrlich ME, et al. Altered synaptic structure in the hippocampus in a mouse model of Alzheimer's disease with soluble amyloid-β oligomers and no plaque pathology. Mol Neurodegener. 2014; 9:41. [PubMed: 25312309]
60. Nunes-Tavares N, Santos LE, Stutz B, Brito-Moreira J, Klein WL, Ferreira ST, et al. Inhibition of choline acetyltransferase as a mechanism for cholinergic dysfunction induced by amyloid-β peptide oligomers. J Biol Chem. 2012; 287:19377–19385. [PubMed: 22505713]
61. Boncristiano S, Calhoun ME, Kelly PH, Pfeifer M, Bondolfi L, Stalder M, et al. Cholinergic changes in the APP23 transgenic mouse model of cerebral amyloidosis. J Neurosci. 2002; 22:3234–3243. [PubMed: 11943824]
62. Van Dam D, Marescau B, Engelborghs S, Cremers T, Mulder J, Staufenbiel M, et al. Analysis of cholinergic markers, biogenic amines, and amino acids in the CNS of two APP overexpression mouse models. Neurochem Int. 2005; 46:409–422. [PubMed: 15737439]
63. Bellucci A, Luccarini I, Scali C, Prosperi C, Giovannini MG, Pepeu G, et al. Cholinergic dysfunction, neuronal damage and axonal loss in TgCRND8 mice. Neurobiol Dis. 2006; 23:260–272. [PubMed: 16766197]
64. Apelt J, Kumar A, Schliebs R. Impairment of cholinergic neurotransmission in adult and aged transgenic Tg2576 mouse brain expressing the Swedish mutation of human β-amyloid precursor protein. Brain Res. 2002; 953:17–30. [PubMed: 12384234]
65. Christensen DZ, Bayer TA, Wirths O. Intracellular Aβ triggers neuron loss in the cholinergic system of the APP/PS1KI mouse model of Alzheimer's disease. Neurobiol Aging. 2010; 31:1153–1163. [PubMed: 18771817]
66. Kar S, Quirion R. Amyloid β peptides and central cholinergic neurons: functional interrelationship and relevance to Alzheimer's disease pathology. Prog Brain Res. 2004; 145:261–274. [PubMed: 14650921]
67. German DC, Yazdani U, Speciale SG, Pasbakhsh P, Games D, Liang CL. Cholinergic neuropathology in a mouse model of Alzheimer's disease. J Comp Neurol. 2003; 462:371–381. [PubMed: 12811807]
68. Nyakas C, Granic I, Halmy LG, Banerjee P, Luiten PG. The basal forebrain cholinergic system in aging and dementia. Rescuing cholinergic neurons from neurotoxic amyloid-beta42 with memantine. Behav Brain Res. 2011; 221:594–603. [PubMed: 20553766]
69. Albuquerque MS, Mahar I, Davoli MA, Chabot JG, Mechawar N, Quirion R, et al. Regional and sub-regional differences in hippocampal GABAergic neuronal vulnerability in the TgCRND8 mouse model of Alzheimer's disease. Front Aging Neurosci. 2015; 7:30. [PubMed: 25852545]
70. Ramos B, Baglietto-Vargas D, del Rio JC, Moreno-Gonzalez I, Santa-Maria C, Jimenez S, et al. Early neuropathology of somatostatin/NPY GABAergic cells in the hippocampus of a PS1xAPP transgenic model of Alzheimer's disease. Neurobiol Aging. 2006; 27:1658–1672. [PubMed: 16271420]

71. Rubio SE, Vega-Flores G, Martinez A, Bosch C, Perez-Mediavilla A, del Rio J, et al. Accelerated aging of the GABAergic septohippocampal pathway and decreased hippocampal rhythms in a mouse model of Alzheimer's disease. FASEB J. 2012; 26:4458–4467. [PubMed: 22835830]

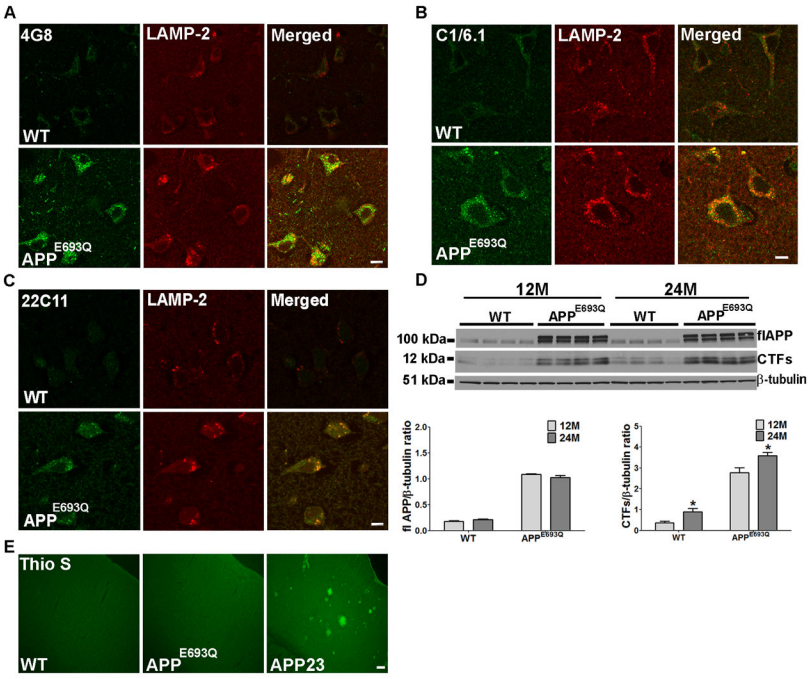

Figure 1. Age-dependent intraneuronal lysosomal accumulation of APP-CTFs and lysosomal abnormality in the brain of APP^{E693Q} mice

Double immunostaining of the entorhinal cortices of 12 months old APP^{E693Q} and WT mice with antibodies to the lysosomal marker LAMP-2 (red) and 4G8 (green), which reacts with flAPP, APP-CTFs, and Aβ (A), with C1/6.1, which reacts with flAPP and APP-CTFs (green) (B), or 22C11 which reacts with flAPP and sAPP (green) (C), (n=4) (Scale bars, 10 μm), revealing intra-lysosomal accumulation of APP-CTFs. (D) Western blot analysis of cerebral homogenates of brains of 12 and 24 months old APP^{E693Q} mice and WT littermate controls using the C1/6.1 antibody revealed an increase in APP-CTFs levels in 24 months old as compared to 12 months old mice. Different exposure times of the same membrane are shown. β-tubulin reactivity is shown as a loading control. Densitometric analysis of the ratio of APP-CTFs signals to β-tubulin. Measurements are presented as the mean ± SEM (n=4/5). The difference among different age groups in mice were significant at *$p<0.05$. (E) Thioflavin-S (Thio-S) staining showing no fibrillar Aβ deposits in the fronto-parietal cortex of APP^{E693Q} mice at 24 months of age as compared to fibrillar Aβ-positive 24 months old APP23 mouse brain (Scale bar, 100 μm).

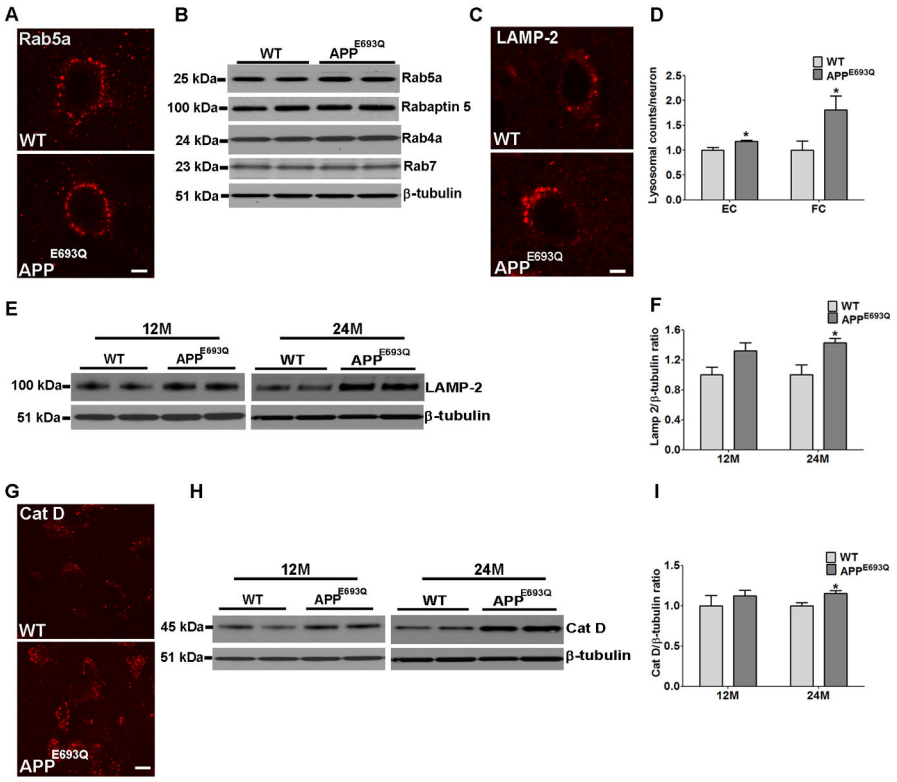

Figure 2. Higher LAMP-2 and Cat D levels in the brain of APP^{E693Q} mice compared to WT control mice

(A) No difference was observed between APP^{E693Q} mice and littermate control neurons immunostained for the early endosomal marker, Rab5, shown here in the frontoparietal cortex (Scale bar, 5 μm). (B) Western blot analysis using anti-Rab4a, Rab5a, Rab7 and Rabaptin 5 antibodies did not show differences in the levels of these proteins in hemibrain homogenates of APP^{E693Q} as compared to WT mice (n=4). (C) Higher signal for LAMP-2 immunoreactivity was observed in the frontoparietal cortex of 12 months old APP^{E693Q} mice compared to age-matched WT controls as found in the entorhinal cortex (Fig 1A-C). (D) Morphometric measurements of LAMP-2 labeled lysosomes revealed higher numbers of lysosomes per neuron in APP^{E693Q} as compared to WT mice. The ratio of LAMP-2 positive lysosomes per neuron in APP^{E693Q} mice was normalized to control mice. (E) Western blot of proteins in the entorhinal cortex of 12 and 24 months old WT and APP^{E693Q} mice, using anti-LAMP-2 antibody. β-tubulin reactivity is shown as a loading control. (F) The ratio of LAMP-2 to β-tubulin reactivity in APP^{E693Q} mice was normalized to control mice. (G) Immunocytochemical staining of the entorhinal cortex of mice at 12 months of age using anti-Cat D antibody (Scale bar, 50 μm). (H) Western blot analysis of homogenates of the entorhinal cortex confirmed higher active Cat D level in 12 and 24 months old APP^{E693Q} mice compared with WT mice. β-tubulin reactivity is shown as a loading control. (I) The ratio of Cat D to β-tubulin reactivity in APP^{E693Q} mice was normalized to control mice. Measurements are presented as the mean ± SEM (n=4/5). The difference from WT mice was significant at *$p<0.05$.

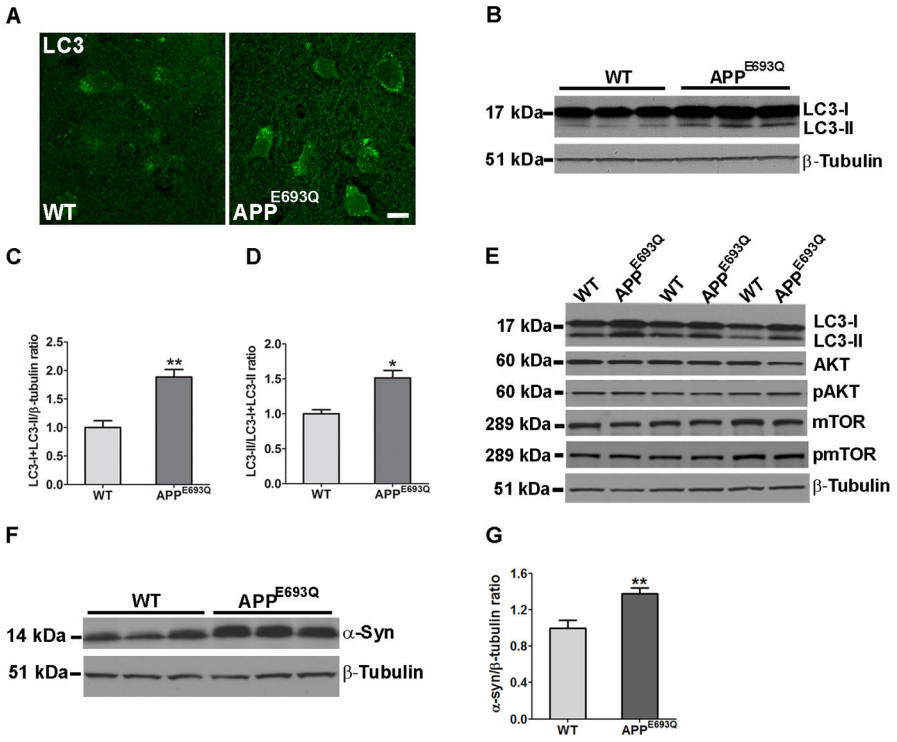

Figure 3. Higher LC3 levels and conversion to LC3-II in the brain of 24 months old APP^{E693Q} mice compared to WT controls

(A) Brain sections immunostained with anti-LC3 antibody showed higher intensity in the entorhinal cortices of APP^{E693Q} as compared to WT mice (Scale bar, 10 μm). (B) Western blot analysis of entorhinal cortical homogenates of APP^{E693Q} as compared to WT mice using an anti-LC3 antibody showed higher intensity of both the LC3-I and LC3-II bands. (C) Quantification of the ratio of total LC3 (LC3-I + LC3-II) to β-tubulin bands in APP^{E693Q} normalized to WT mice, (n=4). (D) Quantification of the ratio of the LC3-II to total LC3 bands in APP^{E693Q} normalized to WT mice, (n=4). (E) Western blot analysis of hemibrain homogenates using anti-LC3, mTOR and AKT antibodies (total and phosphorylated protein) showed higher intensity of both the LC3-I and LC3-II bands in APP^{E693Q} as compared to WT mice whereas no differences were observed in mTOR and AKT expression and phosphorylation levels (n=4). (F) Western blot analysis of brain homogenates showed higher α-synuclein protein levels in hemibrain homogenates of APP^{E693Q} compared with WT mice. (G) Quantification of the ratio of α-synuclein to β-tubulin bands (n=5). All data is presented as the mean ± SEM. The differences from WT mice were significant at *$p<0.05$ and **$p<0.01$.

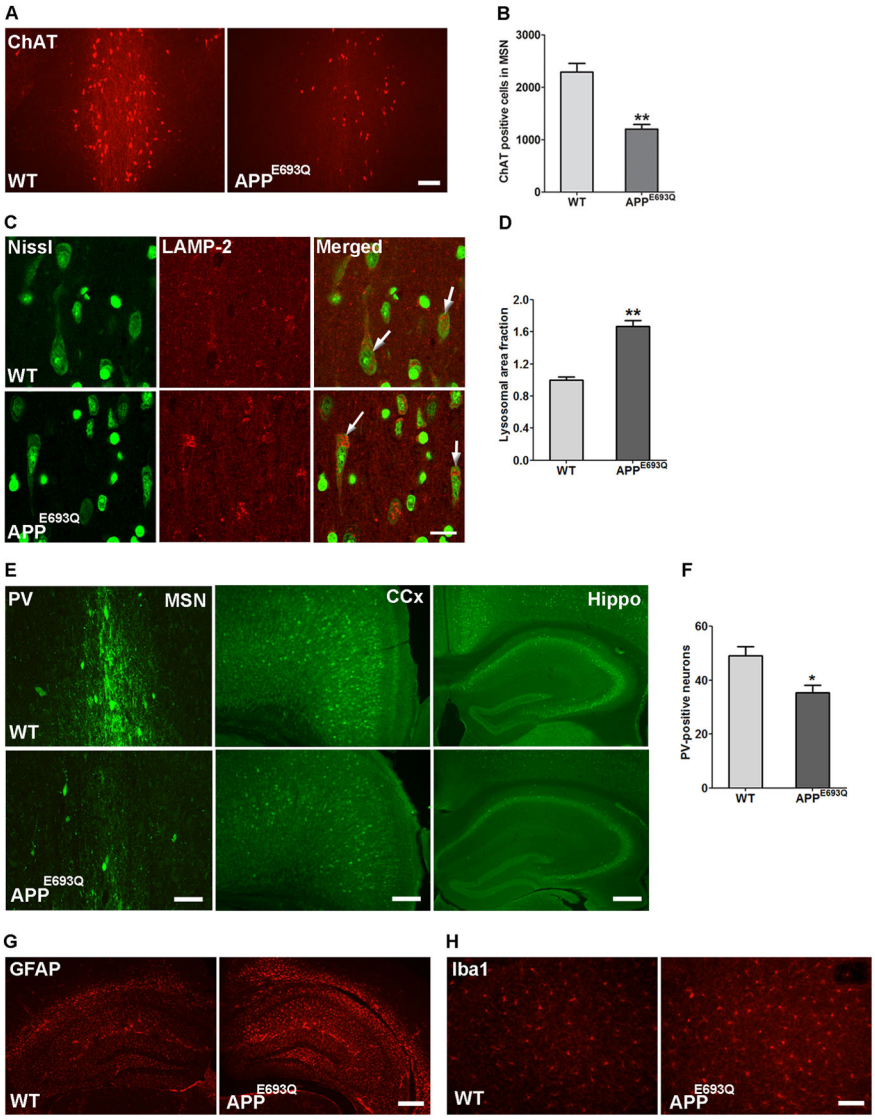

Figure 4. Loss of cholinergic neurons, GABAergic interneurons, and gliosis in the brain of APP^{E693Q} mice at 12 months of age

(A) Loss of ChAT-immuno-positive neurons in the MSN of APP^{E693Q} mice compared to age-matched WT controls (Scale bar, 50 μm). (B) Unbiased stereological quantitation of ChAT-immunopositive cells in the MSN of WT and APP^{E693Q} mice is depicted as cell number ± SEM (n=5). (C) Nissl counter-stained neurons in the MSN of APP^{E693Q} mice immunostained for LAMP-2 showed higher signal for LAMP-2 compared to age-matched WT controls (Scale bars, 20 μm). (D) Morphometric measurements of LAMP-2 labeled lysosomes revealed higher lysosomal area per neuronal area in the Nissl stained large neurons of the MSN (arrowheads) in APP^{E693Q} normalized to WT mice (n=4). (E) Representative pictures of parvalbumin (PV)-positive GABAergic cells in the MSN (scale bar, 50 μm), cingulate cortex (CCx) (scale bar, 100 μm), and hippocampus (Hippo) (scale bar, 200 μm) in WT and APP^{E693Q} mice. (F) Quantification of PV-positive cells in the hippocampus (n=5). (G) Immunocytochemical staining with anti-GFAP antibody of sections

of APP^{E693Q} mouse brains revealed astrogliosis in the hippocampal region as compared to WT mice (Scale bar, 200 μm). (H) APP^{E693Q} mice also exhibited microgliosis in the hippocampal region when immunostained with anti-Iba1 antibody (Scale bar, 50 μm). Differences from WT were significant at *$p<0.05$ and **$p<0.01$.